Published in final edited form as:
Pharmacogenomics. 2004 July ; 5(5): 525–552. doi:10.1517/14622416.5.5.525.

The genomic response of skeletal muscle to methylprednisolone using microarrays: tailoring data mining to the structure of the pharmacogenomic time series

Richard R Almon[1,2], **Debra C DuBois**[1,2], **William H Piel**[1], and **William J Jusko**[2]

1*Department of Biological Sciences, SUNY at Buffalo, Buffalo, NY 14260, USA, Tel: +1 716 645 2363, ext. 114; Fax: +1 716 645 2975; E-mail: almon@eng.buffalo.edu*

2*Department of Pharmaceutical Sciences, SUNY at Buffalo, Buffalo, NY 14260, USA*

Abstract

High-throughput data collection using gene microarrays has great potential as a method for addressing the pharmacogenomics of complex biological systems. Similarly, mechanism-based pharmacokinetic/pharmacodynamic modeling provides a tool for formulating quantitative testable hypotheses concerning the responses of complex biological systems. As the response of such systems to drugs generally entails cascades of molecular events in time, a time series design provides the best approach to capturing the full scope of drug effects. A major problem in using microarrays for high-throughput data collection is sorting through the massive amount of data in order to identify probe sets and genes of interest. Due to its inherent redundancy, a rich time series containing many time points and multiple samples per time point allows for the use of less stringent criteria of expression, expression change and data quality for initial filtering of unwanted probe sets. The remaining probe sets can then become the focus of more intense scrutiny by other methods, including temporal clustering, functional clustering and pharmacokinetic/pharmacodynamic modeling, which provide additional ways of identifying the probes and genes of pharmacological interest.

Keywords

corticosteroids; data mining; expression profiling; gene chips; methylprednisolone; microarrays; modeling; pharmacodynamics; skeletal muscle; time series

Introduction

Synthetic glucocorticoids, corticosteroids, are widely used to suppress inflammatory and immune responses. However, this class of drugs has a low therapeutic index due to a multiplicity of adverse effects on many tissues, including skeletal muscle [1-9]. The adverse effects on skeletal muscle derive from the role of this tissue in glucose homeostasis. One aspect of the broad systemic function of glucocorticoids is to increase gluconeogenesis in the liver and kidney [4,5,10,11]. A primary substrate for gluconeogenesis is amino acid carbon derived from the net degradation of muscle protein. Glucocorticoids also cause muscle to become insulin resistant, thereby preventing the large bulk of the musculature from taking up the glucose produced by the liver and kidney [4,5,12]. When corticosteroids are used therapeutically, their effects on the musculature are accentuated, which results in muscle wasting and insulin-resistant diabetes.

Correspondence to: Richard R Almon.

Corticosteroids produce their effects on skeletal muscle by altering the transcription of specific genes. These transcriptional effects take two fundamental forms, a direct and indirect method. Many regulated genes contain glucocorticoid responsive elements (GREs) in their regulatory sequences and their transcription is influenced directly [2,3,10,13-17]. However, there are a large number of genes whose transcription is altered indirectly by glucocorticoids. In these cases, glucocorticoids alter the expression or function of other transcription factors, which in turn alter the transcription of other genes [13,18-22]. Although still not entirely understood, the phenomena of muscle wasting and insulin resistance clearly involve temporal cascades of changes in the expression of a multiplicity of genes [2-5,19,23-26]. Many genes involved in the phenomena of muscle wasting and insulin resistance have been identified in a piecemeal fashion using diverse *in vitro* and *in vivo* experimental systems. However, understanding such phenomena requires that the temporal cascade of gene expression events be viewed as a whole.

Previously we have used pharmacokinetic/pharmacodynamic (PK/PD) modeling in studies to describe the relationship between bolus dosing with methylprednisolone (MPL) and the change in the expression of a few genes in liver and skeletal muscle [3,10,15-17]. For those experiments, a single bolus dose of MPL was given intravenously to groups of adrenalectomized animals. Animals were sacrificed at 16 time points over a 72-h period. The PK/PD models describe the deviations from and return to baseline (defined by vehicle-treated controls) of gene expression responses. The livers and muscles used for both of these studies were derived from the same animals. Data were analyzed as if samples were taken from a single animal. The data for the change in the expression of mRNA for the PK/PD models was generated using quantitative northern hybridization. Although, more recently, we have converted such measurements to quantitative real-time reverse transcriptase polymerase chain reaction (RT-PCR), even this method does not allow the scope of data collection necessary for developing models for the type of polygenic phenomena initiated by corticosteroids. We previously described the availability of data sets developed by using the Affymetrix GeneChips® Rat Genome (R_U34A) (Affymetrix, Inc., Santa Clara, CA, USA) microarray chip available online, which allows for single gene queries [27]. Those data sets were developed using the same rich time series employed in our earlier studies. The intent was to use gene arrays as a method of high-throughput data collection in order to obtain the scope of data necessary for applying PK/PD modeling to describe broad polygenic phenomena, such as insulin resistance caused by corticosteroids.

Mining such data sets presents uniquely different problems from those encountered when microarrays are used to distinguish one group from another (e.g., cancerous versus non-cancerous tissues). For those applications, one attempts to define a pattern or fingerprint that distinguishes, with very high probability, one group from another [28-33]. In many cases it is the pattern of gene expression rather than the relationship between the genes that is the important focus. In the present application of microarrays, the difficulty lies with sorting through the vast amount of data to identify probe sets with temporal patterns of change in expression, which indicate that the gene is regulated in response to the drug. In this case, the causal relationship between the genes whose expression is changing in response to the drug is of paramount importance. For example, the drug may change the expression of a particular transcription factor, which in turn alters the expression of downstream genes. For this reason the most important aspect of the mining approach is to avoid discarding valuable data. This is of particular importance because each differentially expressed gene becomes the subject of extensive literature searches in order that it can be placed into a temporal context of all other transcriptionally altered genes. The purpose of the endeavor is to use PK/PD modeling to develop a ‘motion picture’ of the polygenic response to the drug.

In the present report we describe a filtering approach to mining the skeletal muscle data set, which is designed to eliminate probe sets that do not meet criteria expected of transcriptionally

altered genes. These criteria are based on our extensive prior knowledge of data for individual genes and their use in PK/PD modeling. This report, therefore, details the small percentage of probe sets in the skeletal muscle data set that meet a specific criteria for further and more intense scrutiny. That same skeletal muscle data set was initially described and its online availability has been detailed in a previous report [27].

Methods and results

Experimental design

Muscle samples (gastrocnemius) were obtained from a previously performed animal study in our laboratory [2,3,10]. Male adrenalectomized (ADX) Wistar rats (*Rattus rattus*) weighing 225–250 g were obtained from Harlan Sprague-Dawley (Indianapolis, IN, USA). Animals were allowed free access to rat chow (Agway, RMH 1000) and 0.9% NaCl drinking water. They were housed in a room with a 12 h light/12 h dark cycle, a constant temperature of 22°C, and were allowed to acclimatize to this environment for at least 1 week. All rats were subjected to right external jugular vein cannulation under light ether anesthesia 1 day prior to the study. Cannula patency was maintained with sterile 0.9% NaCl solution. Four animals were designated as controls (i.e., zero time samples) and received vehicle only. All remaining animals received a single 50 mg/kg dose of MPL sodium succinate (Pharmacia-Upjohn Company, Kalamazoo, MI, USA) via the cannula over 30 s. Rats (3) were sacrificed by exsanguinations under anesthesia at 0.25, 0.5, 0.75, 1, 2, 4, 5, 5.5, 6, 7, 8, 12, 18, 30, 48 and 72 h after dosing. The sampling time points were selected based on previous studies describing glucocorticoid response dynamics and enzyme induction in skeletal muscle and liver. Four cannulated vehicle-treated rats were sacrificed as controls. Gastrocnemius muscles were rapidly excised, flash frozen in liquid nitrogen, and stored at -80°C. Frozen muscle tissues were ground into powder using a liquid-nitrogen-chilled mortar and pestle.

Microarrays

Muscle powder (100 mg) from each individual animal was added to 1 ml of prechilled Trizol® reagent (Invitrogen, Carlsbad, CA, USA) and total RNA extractions were carried out according to the manufacturer's directions. Extracted RNAs were further purified by passage through RNAeasy™ mini-columns (QIAGEN, Valencia, CA, USA) according to the manufacturer's protocols for RNA clean up. Final RNA preparations were resuspended in RNase-free water and stored at -80°C. The RNAs were quantified spectrophotometrically, and purity and integrity were assessed by agarose gel electrophoresis.

Isolated RNA from each individual muscle was used to prepare the target according to the manufacturer's protocols. The biotinylated cRNAs were hybridized to 51 individual R_U34A, which contained 8799 probe sets (in one case, at 30 h, only two samples were available). The Affymetrix arrays used have the advantage of having multiple measurements per gene (≥ 11 probe pairs per transcript). However, this same redundancy leads to many different interpretations of probe sets to determine a signal for each gene (probe set algorithms), and controversy regarding the sensitivity and specificity of resulting signals, as well as appropriate normalization methods [34]. We have used the Affymetrix Microarray Suite (MAS) 5.0® (Affymetrix, Inc., Santa Clara, CA, USA) algorithm, and this places a relatively high penalty for mismatch hybridization, favoring specificity over sensitivity [35]. This entire data set has been submitted to the National Center for Biotechnology Information (NCBI) Gene Expression Omnibus database (GSE490) and is also available online [27,101].

Data analysis

The approach to data mining was developed based on our use of gene arrays as a technique for high-throughput data collection within the context of a rigidly controlled time series paradigm.

The Affymetrix oligonucleotide microarrays use sequence information and photolithography-directed combinatorial chemical synthesis to develop probe sets for the genes of interest. Each probe set consisted of a series of short oligonucleotide sequences and an identical partner sequence, except for a single base mismatch in the center. The mismatch sequence provided a unique background for each sequence in the series. MAS 5.0 was used for initial data acquisition and basic analysis. In this first step, a 'call' of present (P), absent (A) or marginal (M) was determined for each probe set on each chip based on the comparison of the matched and mismatched pairs for the gene sequence. The results were normalized for each chip using a distribution of all genes around the 50th percentile. The results from the first step were entered into the program GeneSpring 6.1® (Silicon Genetics, Redwood City, CA, USA). This robust software provides a number of tools for visualization and analysis of time series data. One such tool for both hierarchical clustering and visualization is the gene tree approach described by Eisen [36] as modified by the Gene-Spring software. This algorithm can be used to construct a dendrogram of genes with similar patterns. A negative aspect of this tool, and most time series data-mining tools, is the assumption that the points in the time series are equally spaced. However, to design our 72 h time series in this manner would have ignored the richness of biological information during the early period following dosing of the drug. Notwithstanding this drawback, gene trees provide an excellent method of visualizing the progression of the data analysis. In order for this and other tools to be used it was also necessary to transform the data so that the values for all probe sets were within the same range. To accomplish this, values for each individual probe set on each chip were expressed as a ratio of the mean of the four control values for that gene, which we refer to as 'normalized intensity'. Thus, the average of each probe set has a value of 1 at zero time and either increases, decreases or remains unchanged relative to controls over the time series.

Figure 1 (top left) shows the gene tree derived from the Genespring program for the entire data set (8799 probe sets at 17 time points). This tree was constructed with the program's default method, which uses Pearson correlation around zero. The x-axis presents the 17 time points studied in rank order from left to right. Vehicle controls are nominally referred to as time zero. As pointed out above, each time point is equally spaced and, therefore, does not represent the true temporal relationship between points. The y-axis presents the mean of the normalized value at each time point for each of the individual probe sets, represented by color and clustered by similarity. In this view, the color yellow represents a value of '1', progression toward red represents values that exceed '1', and progression toward blue represents values that decline toward 0. The intensity of the color reflects the intensity of the original signal. To the immediate left of the gene tree is a schematic tree of the relationship of all probe sets to each other based on expression pattern similarity (represented in green). On the left side of the gene tree, but spatially separated, is what is referred to as a 'marquee view' in the GeneSpring software. This marquee view can be used to navigate the view of the main gene tree. Although the gene tree representation of the entire data set is of limited value for examining individual gene patterns of regulation, it does illustrate two points. First, within the entire data set there are a vast number of genes represented by black (no expression in skeletal muscle regardless of treatment) or by the color yellow across the entire time frame studied. This latter group of genes exhibits no temporal regulation by the drug (i.e., their expression does not deviate from control value following drug dosing) and represents the probe sets that we wish to filter from the data set. This gene tree does reflect segregation of similarly regulated genes and demonstrates that similar patterns of regulation do exist. For example, groups of intense red or blue represent clusters of genes with similar up- or downregulation, respectively. Figure 1 (top right) provides a magnified view of one such clustering of upregulated probe sets. The location of this group of probe sets on the entire gene tree is indicated by the white bracket. Figure 1 (bottom) shows an even closer zoom in on five probe sets in this grouping with similar patterns. In this case, two probe sets for the gene regenerating liver inhibitory factor-1 (RL/IF-1) (*X63594*) segregate

next to each other, which demonstrates the optimal function of gene tree clustering. The location of these probe sets in the top right panel is indicated by the white rectangle.

A series of 'filtering' steps were applied to the data in an attempt to identify genes and eliminate probe sets that either are not expressed in skeletal muscle or are not responsive to MPL treatment. The first level of filtering was designed to eliminate probe sets not expressed in skeletal muscle regardless of drug treatment (represented by a very low intensity on the gene tree), and utilized the Affymetrix 'call' feature. For this step we explored two different levels of stringency. The first approach that we employed required the probe set for the gene to have a call of P on at least 25 of the 51 chips. This filter reduced the number of remaining probe sets from the original 8799 to 3785. We compared this result with a less stringent filter that only required a call of P on 4 of the 51 chips. This filter reduced the number of remaining probe sets from the original 8799 to 4636. This endeavor identified two types of probe sets that would be lost by greater stringency at this step. The first was a group of probe sets that started below the sensitivity of the chip (background) then appeared on a contiguous sets of chips in which the call was P that then returned to a series of A chip calls. The second was a group of probe sets that initially had calls of P but, following dosing, dropped to A for a period of time before returning to a call of P. We chose not to exclude these probe sets with this initial filter because it appeared that the drug treatment was influencing the quality call of the probe set by the software, thus suggesting possible regulation. A final observation concerning the background is that there is considerable variation in the probe set backgrounds on the R_U34A chip. Some probe sets can obtain a call of P with a signal as low as 10 units while others require a signal > 350 units. As our major concern was to prevent discarding valuable data, we chose the less stringent 4P filter for this initial filtering step. Figure 2 provides a gene tree of the 4636 probe sets not eliminated by this filter. Thus, requiring that a signal be present on only four chips eliminated > 4000 probe sets.

The second level of filtering was designed to eliminate probe sets that could not meet the basic criteria of a regulated probe. Specifically, this filter was designed to eliminate probe sets whose average did not deviate from baseline by a certain value for a reasonable number of time points. After exploring a variety of filtering values and number of conditions using gene trees in the manner described in the previous paragraph, we developed two filters that were designed to eliminate probe sets that were neither down- nor upregulated. The first filter eliminated probe sets that could not meet a minimal criteria for down-regulation. Starting with the 4P filtered list we eliminated all probe sets that did not have average values < 0.65 in at least four conditions (time points). Figure 3 (top left) shows a gene tree of the 354 probe sets that were not eliminated by this filter. Most of these probe sets clearly contain a sustained run of time points represented by the color blue, as expected of downregulated probe sets. The next filter was designed to eliminate probe sets that could not meet a minimal criterion for upregulation. Starting with the 4P filtered list, we eliminated all probe sets that did not have average values > 1.5 in at least four conditions (time points). Figure 3 (top right) shows a gene tree of the 349 probe sets that were not eliminated by this filter. Most of these probe sets clearly contain a sustained run of red time points as expected of upregulated probe sets. There were a small number of probe sets that were not eliminated by either filter indicating both up- and downregulation. These probe sets (which were present on both lists) suggest biphasic regulation, a phenomenon we have previously described [13]. Figure 3 (bottom) shows a gene tree of the 690 probe sets that were not eliminated by any of the filters applied. Thus, using four straightforward filters, we were able to eliminate all but 8% of the probe sets present in the original data set.

The last non-statistical filter we applied addressed the quality of the data. For this 'quality control' filter we eliminated probe sets that did not meet one of two conditions. The first condition focused on the control chips. As indicated above, our initial operation was to divide the value of each individual probe set on each chip by the mean of the values for that probe set

on the four control chips. Therefore, the quality of the control data for each particular probe set is of paramount importance in defining regulation by the drug. The second condition focused on the remaining 16 time points. Using the standard deviation of the mean, this filter excluded all probe sets whose coefficient of variation (CV) for the control chips exceeded 50% or whose CV for > 8 of the remaining 16 time points exceeded 50%. For the one time point in which only two samples were available (30 h), a quasi-CV was calculated by dividing the difference between the two values by the average. This 'quality control' filter eliminated an additional 37 probe sets. Figure 4 (left) provides a gene tree of the 653 probe sets that were not eliminated by the entire series of filters. Figure 4 (right) shows the 8146 probe sets that were filtered out by the entire set of filters. Comparing Figure 1 (top left) with Figure 4 (right) demonstrates that probes with apparent regulation are no longer present in the total data set. The 653 probe sets remaining after filtering the total data set (Figure 4, left) are the product of this approach to data mining and, thus, become the focus of temporal clustering, functional clustering, and PK/PD modeling.

Our previous work demonstrated that three basic temporal signatures of regulation can be expected following single bolus dosing by MPL of a population of ADX rats that have a stable baseline. These three signatures indicate upregulation, downregulation, and biphasic regulation. Figure 5 top left (313 probe sets), top right (321 probe sets), and bottom (19 probe sets) provide gene trees for probe sets that fall into these three categories respectively. As a final evaluation of the results we performed a 1-way analysis of variance (ANOVA) with a Tukey post-hoc test ($p < 0.05$) on each of the three groups. Tables 1, 2 and 3 list the probe sets in these three groups, respectively. The ANOVA identified for exclusion 62 of 313 probe sets from Table 1, 95 of 321 probe sets from Table 2 and 2 of 19 probe sets from Table 3. Those probe sets identified for exclusion by the ANOVA are highlighted in the tables.

Discussion

A population of ADX male Wistar rats was injected with a single bolus dose of MPL, groups of three animals were sacrificed at 16 time points over a 72-h period, and MPL-treated samples were compared with vehicle-treated controls. ADX animals were used to eliminate the circadian oscillation of corticosterone and provide a stable baseline [2,3,10,15-17]. This allowed us to identify gene transcripts that deviate from the baseline in response to MPL, and determine the duration of time it takes to return to that baseline. The times of sacrifice over the 72-h period were chosen based on previous experiments, which indicated that the effect of the drug was most significant soon after dosing but, in some cases, full recovery required as long as 72 h.

R_U34A chips were used to examine the temporal profile of changes in global gene expression in skeletal muscle in response to this single bolus dose of MPL. RNA samples from each individual animal were applied to a separate chip to preserve inter-animal variation. As this chip contains 8799 probe sets, the major problem was identifying the small percentage of the probe sets that are regulated by corticosteroids. In previous work, we have used cluster analysis tools to concurrently address the problems of data mining and temporal clustering with a similar data set developed using the livers from these animals [13]. Those tools did identify several subgroups of regulated probe sets. However, while examining genes in the pathways we were prompted to visually inspect the results for genes that 'should' have been regulated based on the literature. The results of the visual inspection of individual genes demonstrated to us that the initial very stringent approach that we employed eliminated probe sets that were clearly regulated. There are two reasons for this deficit. First, we approached data mining (identifying regulated probe sets) and clustering as a single process using clustering algorithms based on Euclidian distance and correlation coefficients. Neither Euclidian distance nor correlation coefficients incorporate time interval. In our time series design, 9 of the 16 points are within

the first 6 h and 12 of the 16 points are within the first 12 h. The interval between time domains ranged from 0.25 h in the beginning to 24 h at the end. Our previous use of Self Organizing Maps (SOM) and K-means, which are based on Euclidian distance, did not consider varying time interval in the analysis. Our subsequent application of correlation coefficients did not rectify the problem. We, therefore, developed a new approach to data mining that is based on a series of filters designed to eliminate probe sets that do not meet certain explicit criteria. This series of filters produces a small percentage of the total probe sets, which can then become the focus of temporal and functional clustering. The latter will then provide an additional filter prior to applying the ultimate objective, mechanism-based PK/PD modeling. Since we have previously published data on expression changes of small groups of genes measured individually by other methods in conjunction with PK/PD modeling of that data, the drug kinetics and receptor dynamics for this data set have been published [3,10]. When such models are developed, one aspect is to evaluate the goodness of fit of the data to the model.

The basis of this new approach is to filter the database based on specific characteristics of the probe sets that we wished to be eliminated. The first filter we applied was designed to eliminate all probe sets that were not expressed in skeletal muscle. This filter reduced the number of probe sets under consideration from 8799 to 4636. The second filter we applied was designed to identify and eliminate a group of probe sets that do not meet the criteria of downregulation. This filter eliminated all but 354 probe sets. Similarly, we filtered the remaining 4282 probe sets for those that did not meet a minimum criteria for upregulation. This filter eliminated all but 349 probe sets.

HIghlights

- Microarrays provide a method for the type of high-throughput data collection necessary for mechanism-based PK/PD modeling of complex biological systems.
- A time series is able to capture the cascades of molecular events commonly initiated by drug dosing.
- Data mining a drug response microarray time series involves sorting through a massive amount of data. A rational approach to this problem is to eliminate, by using defined and relevant filters, those probe sets that do not meet minimum criteria for expression in the tissue, regulation by the drug, and data quality.
- Those probe sets that are not eliminated by these filters can then become the subject of temporal clustering, functional clustering, and PK/PD modeling.

We then combined the two lists of probe sets that had not been eliminated and filtered that list of 690 probe sets on data quality. The results of the entire set of filters is that 8146 probe sets of the original 8799 probe sets were eliminated from further consideration. This left a remainder of 653 probe sets for further consideration with respect to temporal clustering, functional clustering, and PK/PD modeling.

The use of a rich time series of expression microarrays as a high-throughput method of data collection provides a means for obtaining the patterns of differential expression necessary for developing PK/PD models for complex phenomena, such as steroid-induced insulin resistance or muscle wasting. The initial problem presented by this approach is the necessity to focus attention on a small percentage of regulated genes out of the thousands measured by gene arrays. Probes that fit this category should meet minimal requirements, such as being expressed in the tissue and deviating from baseline for a period of time. They should also meet certain data quality criteria. The series of filters applied to the present data set eliminated > 92% of the probe sets in a simple, straightforward manner. It should be pointed out that this filtration

approach takes advantage of the richness of the time series. As this entire data set is available online in a single gene query format [27], the present report makes the subset of probes that warrant further consideration generally available, along with their criteria of selection.

Outlook

In the future, the focus in pharmacogenomics will increasingly shift away from simply identifying genes whose expression is altered by a particular drug toward modeling the dynamic relationship between the elements in the cascade of events in the complex biological system. In the case of skeletal muscle and the response to corticosteroids, such models will allow us to begin to address questions such as dosing regimen and the development of polygenic adverse effects, including insulin resistance and atrophy. These transcriptional models will also provide the scaffolding onto which translational and post-translational data can be placed.

Acknowledgements

This work was supported by grants GM 24211 and 1 P20 GM67650 from the National Institute of General Medical Sciences, NIH. This data set was developed under the auspices of a grant from the National Heart, Lung, and Blood Institute (NHLBI)/NIH Programs in Genomic Applications U01 HL66614.

Bibliography

Papers of special note have been highlighted as either of interest (•) or of considerable interest (••) to readers.

1. Almon RR, DuBois DC. Fiber-type discrimination in disuse and glucocorticoid-induced atrophy. Med Sci Sports Exerc 1990;22:304–311. [PubMed: 2199752]
2. McKay LI, DuBois DC, Sun YN, Almon RR, Jusko WJ. Corticosteroid effects in skeletal muscle: gene induction/receptor autoregulation. Muscle Nerve 1997;20:1318–1320. [PubMed: 9324091]
3. Sun YN, McKay LI, DuBois DC, Jusko WJ, Almon RR. Pharmacokinetic/pharmacodynamic models for corticosteroid receptor down-regulation and glutamine synthetase induction in rat skeletal muscle by a receptor/gene-mediated mechanism. J Pharmacol Exp Ther 1999;288:720–728. [PubMed: 9918581]•• Provides receptor dynamics and drug kinetics for this data set, as well as PK/PD models of selected genes in skeletal muscle.
4. Reynolds RM, Walker BR. Human insulin resistance: the role of glucocorticoids. Diabetes Obes Metab 2003;5:5–12. [PubMed: 12542720]
5. Selyatitskaya VG, Kuzminova OI, Odintsov SV. Development of insulin resistance in experimental animals during long-term glucocorticoid treatment. Bull Exp Biol Med 2002;133:339–341. [PubMed: 12124639]
6. Wald JA, Farr RS. Abnormal liver-function tests associated with long-term systemic corticosteroid use in subjects with asthma. J Allergy Clin Immunol 1991;88:277–278. [PubMed: 1880328]
7. Eisenstein A. Effects of adrenal cortical hormones on carbohydrate, protein, and fat metabolism. Am J Clin Nutr 1973;26:113–120. [PubMed: 4345514]
8. Tomono S, Ohyama Y, Uchiyama T. Insulin resistance induced by drugs, inflammation and stress. Jpn J Clin Med 2002;60:632–636.
9. Bialas MC, Routledge PA. Adverse effects of corticosteroids. Adverse Drug React Toxicol Rev 1998;17:227–235. [PubMed: 10196628]
10. Sun YN, DuBois DC, Almon RR, Jusko WJ. Fourth-generation model for corticosteroid pharmacodynamics: a model for methylprednisolone effects on receptor/gene-mediated glucocorticoid receptor down-regulation and tyrosine aminotransferase induction in rat liver. J Pharmacokinet Biopharm 1998;26:289–317. [PubMed: 10098101]• A more detailed description of the animals used in this study, as well as PK/PD models of selected genes in liver.
11. Almon RR, DuBois DC, Brandenburg EH, et al. Pharmacodynamics and pharmacogenomics of diverse receptor-mediated effects of methylprednisolone in rats using microarray analysis. J Pharmacokinet Pharmacodyn 2002;29:103–129. [PubMed: 12361239]

12. Barbera M, Fierabracci V, Novelli M, et al. Dexamethasone-induced insulin resistance and pancreatic adaptive response in aging rats are not modified by oral vanadyl sulfate treatment. Eur J Endo 2001;145:799–806.

13. Jin JY, DuBois DC, Jusko WJ, Almon RR. Modeling of corticosteroid pharmacogenomics in rat liver using gene microarrays. J Pharmacol Exp Ther 2003;307:93–109. [PubMed: 12808002]•• Provides our initial clustering approach applied to a liver data set developed from the same animals, and pharmacogenomic modeling of selected genes from that data set.

14. Klaassen CD. Induction of metallothionein by adrenocortical steroids. Toxicology 1981;20:275–279. [PubMed: 7314118]

15. Ramakrishnan R, DuBois DC, Almon RR, Pyszczynski NA, Jusko WJ. Fifth-generation model for corticosteroid pharmacodynamics: application to steady-state receptor down-regulation and enzyme induction patterns during seven-day continuous infusion of methylprednisolone in rats. J Pharmacokinet Pharmacodyn 2002;29:1–24. [PubMed: 12194533]

16. Ramakrishnan R, DuBois DC, Almon RR, Pyszczynski NA, Jusko WJ. Pharmacodynamics and pharmacogenomics of methylprednisolone during 7-day infusions in rats. J Pharmacol Exp Ther 2002;300:245–256. [PubMed: 11752123]

17. Sun YN, DuBois DC, Almon RR, Pyszczynski NA, Jusko WJ. Dose-dependence and repeated-dose studies for receptor/gene-mediated pharmacodynamics of methylprednisolone on glucocorticoid receptor down-regulation and tyrosine aminotransferase induction in rat liver. J Pharmacokinet Biopharm 1998;26:619–648. [PubMed: 10485078]

18. Garlatti M, Aggerbeck M, Bouguet J, Barouki R. Contribution of a nuclear factor 1 binding site to the glucocorticoid regulation of the cytosolic aspartate aminotransferase gene promoter. J Biol Chem 1996;271:32629–32634. [PubMed: 8955092]

19. Long W, Wei L, Barrett EJ. Dexamethasone inhibits the stimulation of muscle protein synthesis and PHAS-I and p70 S6-kinase phosphorylation. Am J Physiol Endocrinol Metab 2001;280:E570–E575. [PubMed: 11254463]

20. Makkinje A, Quinn DA, Chen A, et al. Gene 33/Mig-6, a transcriptionally inducible adapter protein that binds GTP-Cdc42 and activates SAPK/JNK. A potential marker transcript for chronic pathologic conditions, such as diabetic nephropathy Possible role in the response to persistent stress. J Biol Chem 2000;275:17838–17847. [PubMed: 10749885]

21. Masters JN, Cotman SL, Osterburg HH, Nichols NR, Finch CE. Modulation of a novel RNA in brain neurons by glucocorticoid and mineralocorticoid receptors. Neuroendocrinology 1996;63:28–38. [PubMed: 8839352]

22. Takiguchi M, Mori M. Transcriptional regulation of genes for ornithine cycle enzymes. Biochem J 1985;312:649–659. [PubMed: 8554501]

23. Bodine SC, Latres E, Baumhueter S, et al. Identification of ubiquitin ligases required for skeletal muscle atrophy. Science 2001;294:1704–1708. [PubMed: 11679633]

24. Son C, Hosoda K, Matsuda J, et al. Up-regulation of uncoupling protein 3 gene expression by fatty acids and agonists for PPARs in L6 myotubes. Endocrinology 2001;142:4189–4194. [PubMed: 11564673]

25. Sugden MC, Orfali KA, Holness MJ. The pyruvate dehydrogenase complex: nutrient control and the pathogenesis of insulin resistance. J Nutr 1995;125:1746S–1752S. [PubMed: 7782939]

26. Sugden MC, Holness MJ. Therapeutic potential of the mammalian pyruvate dehydrogenase kinases in the prevention of hyperglycaemia. Curr Drug Targets Immune Endocr Metab Disord 2002;2:151–165.

27. Almon RR, Chen J, Snyder G, DuBois DC, Jusko WJ, Hoffman EP. *In vivo* multi-tissue corticosteroid microarray time series available online at Public Expression Profile Resource (PEPR). Pharmacogenomics 2003;4:791–799. [PubMed: 14596642]•• Description of and online access to this dataset.

28. Cojocaru G, Friedman N, Krupsky M, et al. Transcriptional profiling of non-small cell lung cancer using oligonucleotide microarrays. Chest 2002;121:44S. [PubMed: 11893681]

29. Friedman, N.; Kaminski, N. Statistical methods for analyzing gene expression data for cancer research. Ernst Schering Res. Found. Workshop; 2002. p. 109-131.

30. Kaminski N. Microarray analysis of idiopathic pulmonary fibrosis. Am J Respir Cell Mol Biol 2003;29:S32–S36. [PubMed: 14503551]

31. Lock C, Hermans G, Pedotti R, et al. Gene-microarray analysis of multiple sclerosis lesions yields new targets validated in autoimmune encephalomyelitis. Nat Med 2002;8:500–508. [PubMed: 11984595]

32. Morgan KT, Ni H, Brown HR, et al. Application of cDNA microarray technology to *in vitro* toxicology and the selection of genes for a real-time RT-PCR-based screen for oxidative stress in Hep-G2 cells. Toxicol Pathol 2002;30:435–451. [PubMed: 12187936]

33. Rhodes DR, Barrette TR, Rubin MA, Ghosh D, Chinnaiyan AM. Meta-analysis of microarrays: interstudy validation of gene expression profiles reveals pathway dysregulation in prostate cancer. Cancer Res 2002;62:4427–4433. [PubMed: 12154050]

34. Tumour Analysis Best Practices Working Group. Expression profiling – best practices for data generation and interpretation in clinical trials. Nat Rev Genet 2004;5:229–237. [PubMed: 14970825] • Provides a discussion of various probe set algorithms.

35. Seo J, Bakay M, Chen Y, Himler S, Shneiderman B, Hoffman E. Optimizing signal/noise ratios in expression profiling, project-specific algorithm selection and detection p value weighting in affymetrix microarrays. Bioinformatics. 2004In Press•• A discussion of the utility of MAS 5.0 probe set algorithm.

36. Eisen MB, Spellman PT, Brown PO, Botstein D. Cluster analysis and display of genome-wide expression patterns. Proc Natl Acad Sci USA 1998;95:14863–14868. [PubMed: 9843981]•• Original description of the gene tree approach for clustering.

Website

101. http://microarray.cnmcresearch.org/pgadatatable.asp Microarray Center Homepage.

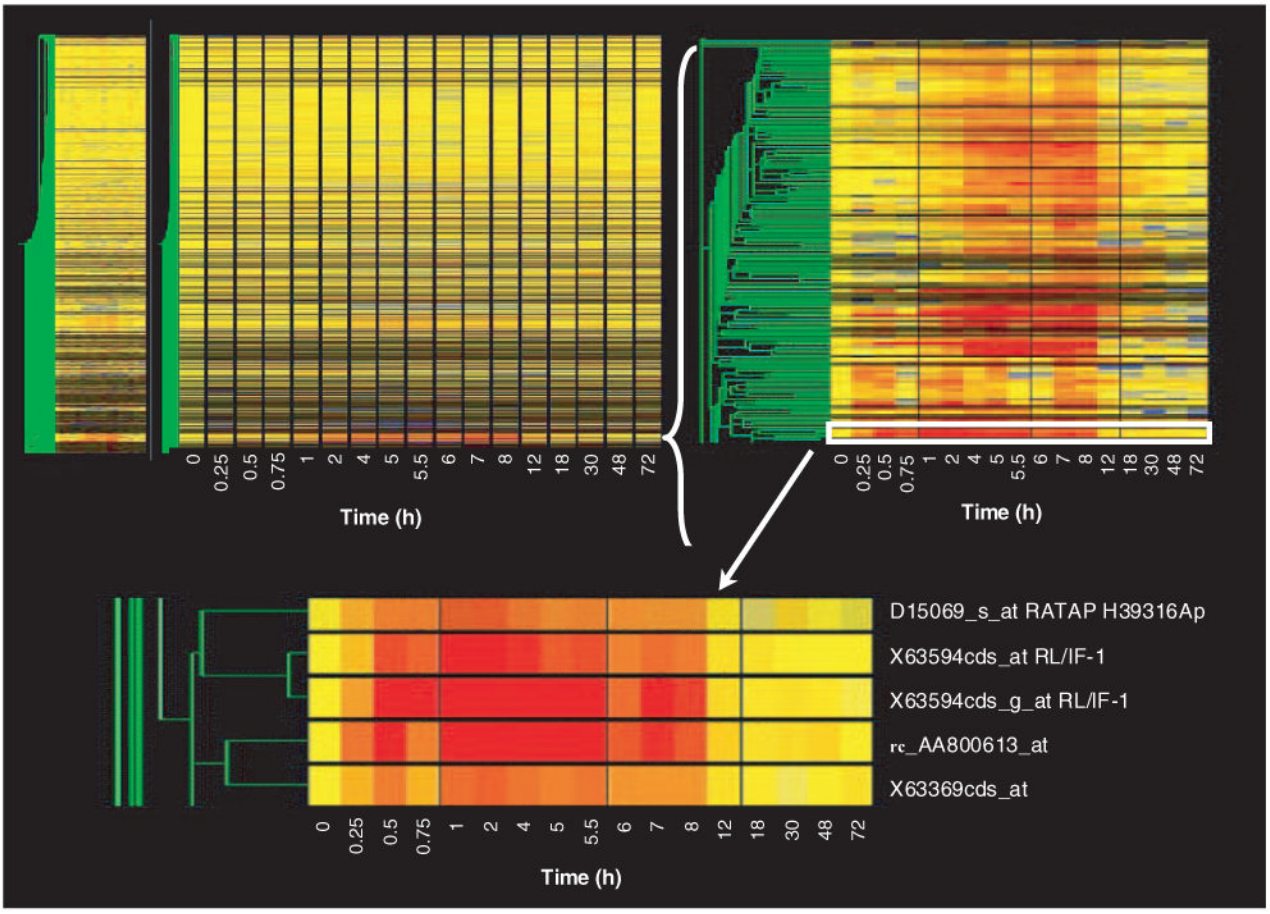

Figure 1. Gene tree representation of an entire data set of mRNA expression in skeletal muscle as a function of time following methylprednisolone treatment

The gene tree represents the averaged normalized values of each of 8799 probe sets at 17 different time points following methylprednisolone treatment, grouped by pattern similarities. The y-axis represents individual probe sets, with color representing relative intensities (yellow represents no change from control, progression toward red indicates increased expression, and progression toward blue represents decreased expression versus control values). The x-axis ranks the samples in sequence of time following methylprednisolone treatment. The top left panel represents the entire data set, while the top right and bottom panels present successively magnified views of the areas highlighted.

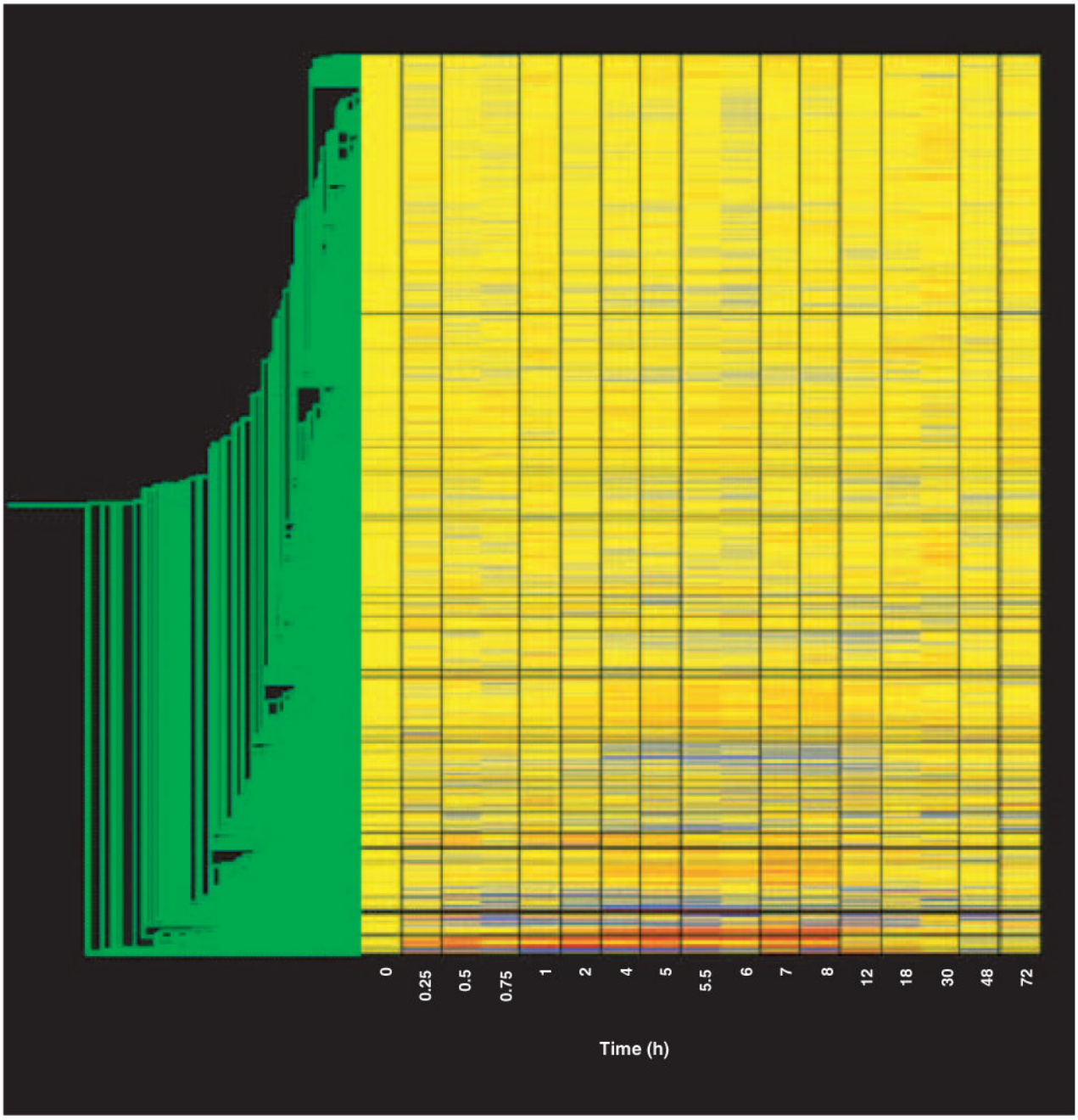

Figure 2. Gene tree of the 4636 probe sets remaining after filtering to remove probe sets not expressed in skeletal muscle regardless of drug treatment

Gene tree of probe sets remaining after filtering as described in the text. The gene tree is as described in Figure 1.

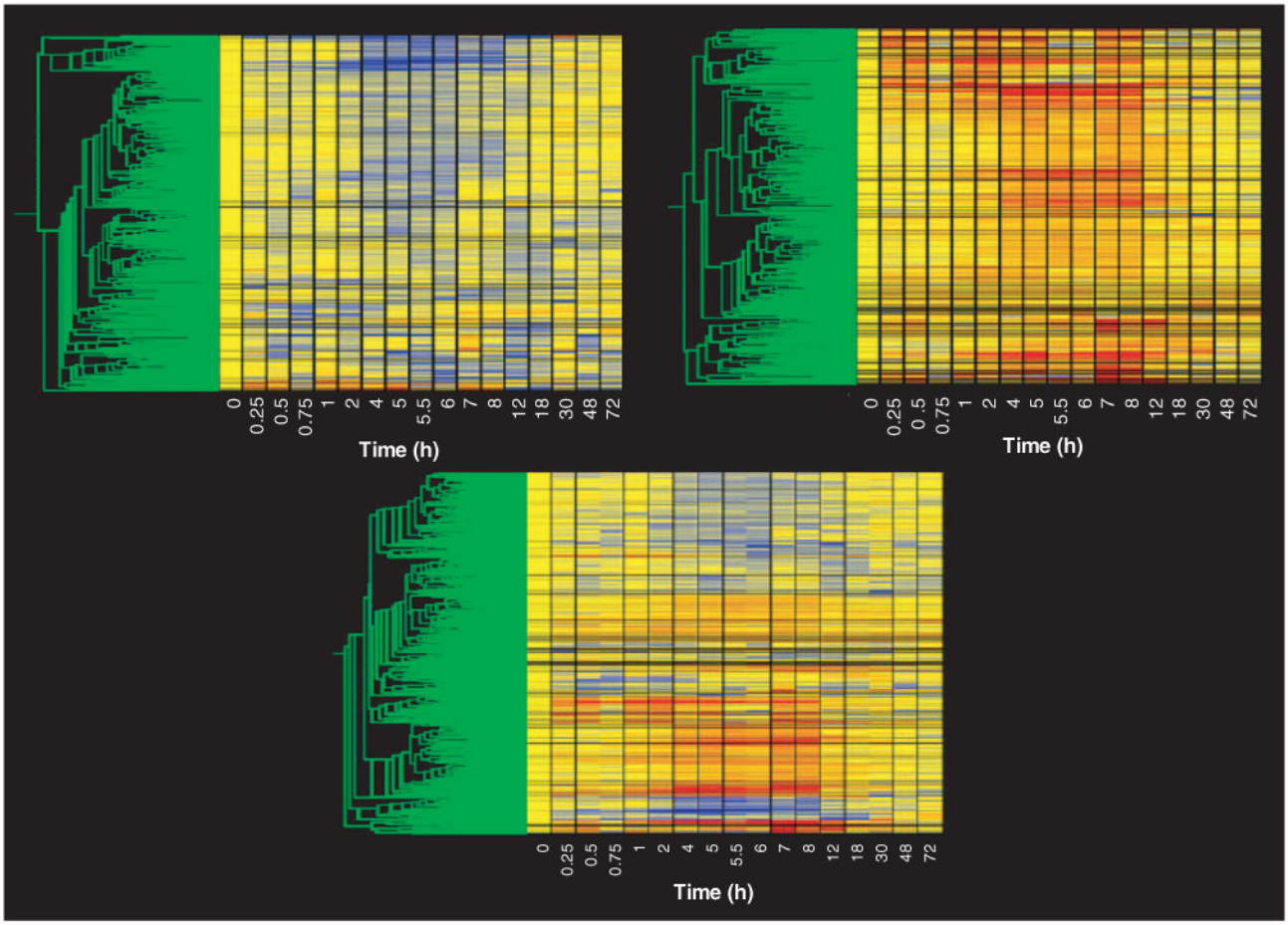

Figure 3. Gene tree of probe sets remaining following filtering for non-drug-regulated probe sets

The top left panel presents the 354 probe sets remaining after filtering out probe sets not exhibiting repressed expression, as described in the text. The top right panel presents the 349 probe sets remaining after filtering out probe sets not exhibiting enhanced expression, as described in the text. The bottom panel presents all probe sets not eliminated by either filtering step recombined into a single gene tree. A description of the gene tree is provided in Figure 1.

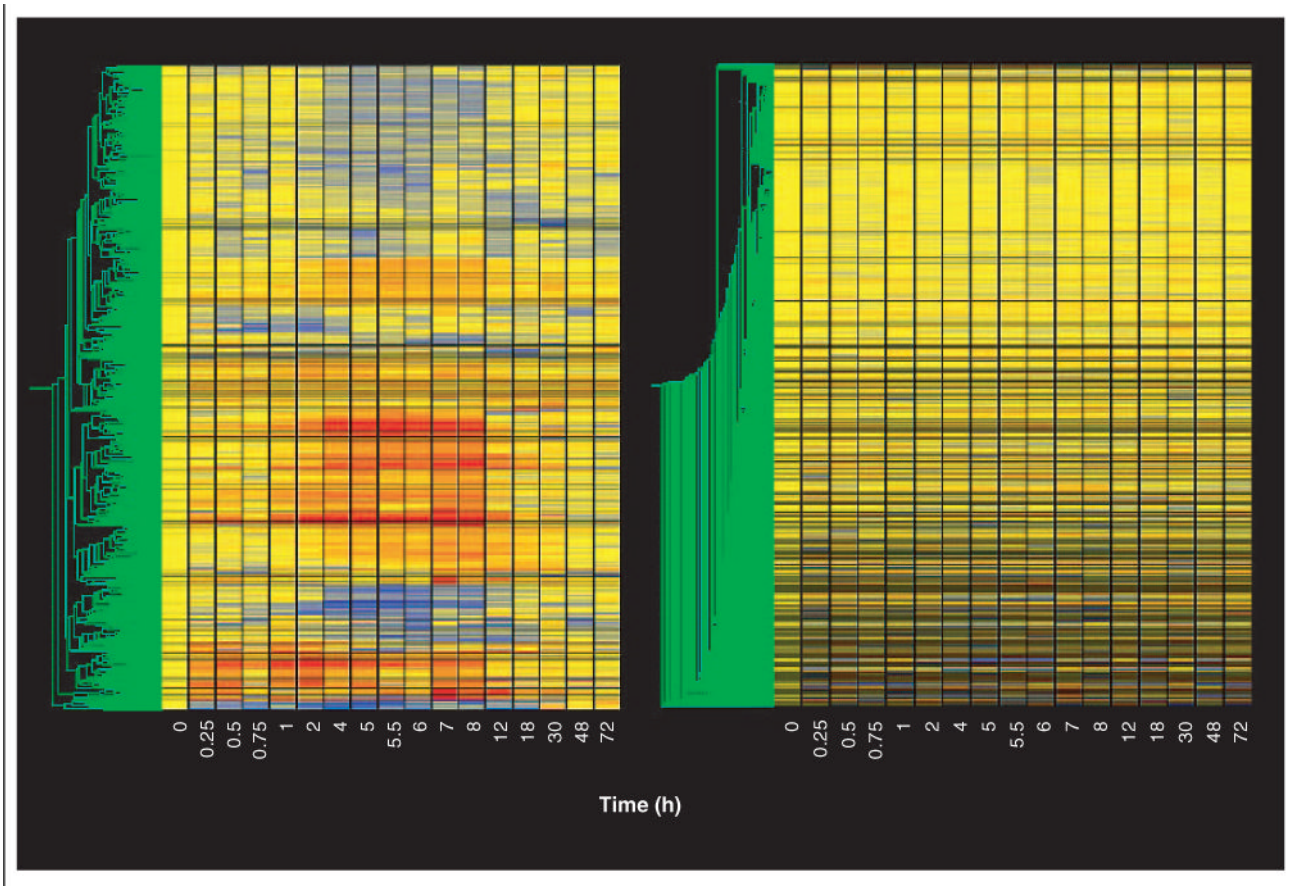

Figure 4. Gene trees of the remaining probe sets after completion of all filtering steps and of the eliminated probe sets

Gene trees of the 653 probe sets remaining after completion of all filtering steps described in the text (left panel), and of the 8146 eliminated probe sets (right panel). Gene trees are as described in Figure 1.

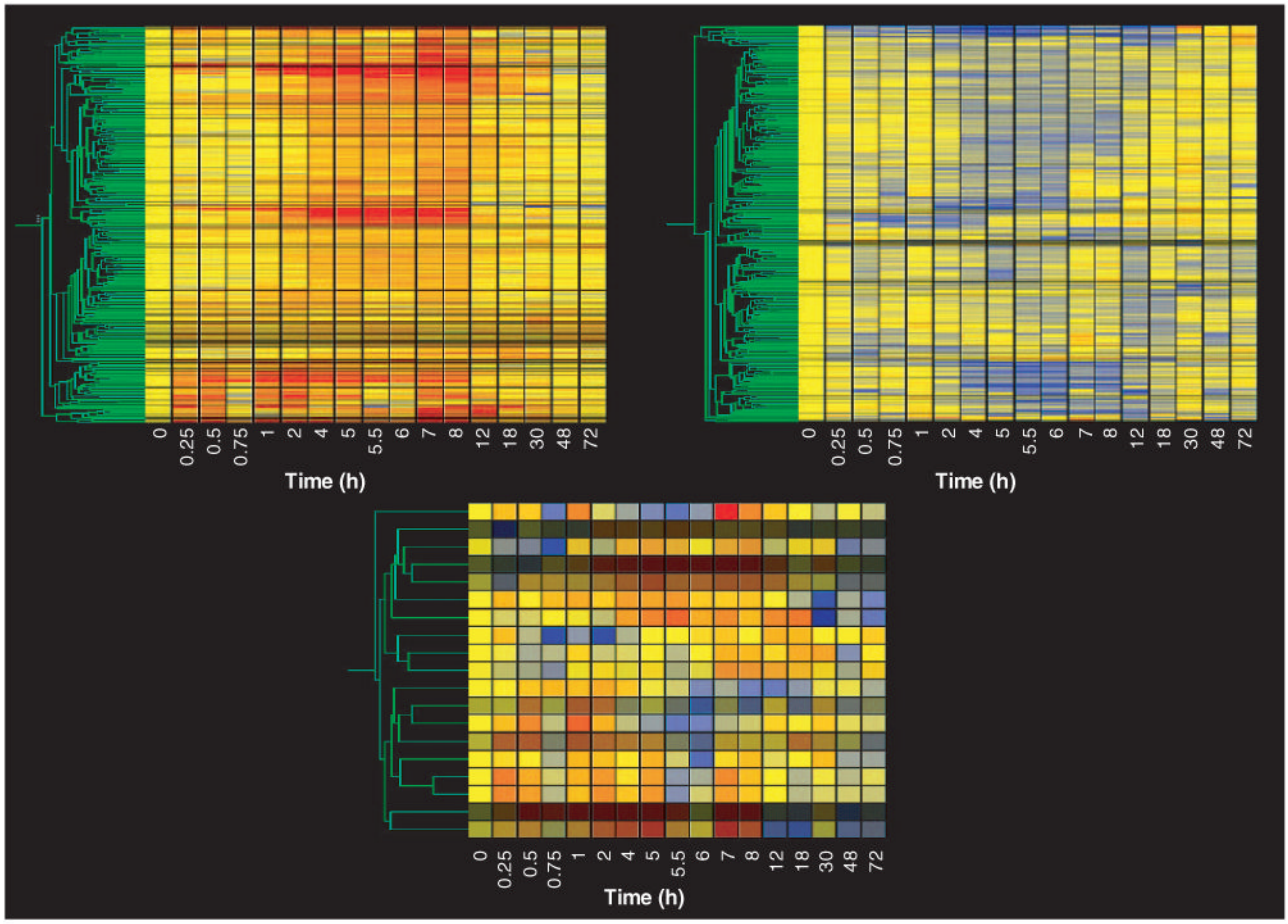

Figure 5. Gene trees of probe sets representing upregulation, downregulation and biphasic regulation in skeletal muscle as a function of time following methylprednisolone administration

Gene trees of probe sets representing upregulation (top left), downregulation (top right) and biphasic regulation (bottom) in skeletal muscle as a function of time following methylprednisolone administration. Gene trees are as described in Figure 1.

Table 1

Upregulated probe sets

Probe set ID	Gene name
D45920_at	130-kDa-Ins(1,4,5)P3-binding protein
rc_AI072447_s_at	130-kDa-Ins(1,4,5)P3-binding protein
M33648_g_at	3-Hydroxy-3-methylglutaryl-coenzyme A synthase 2
Y15748_at	3-Phosphoinositide-dependent protein kinase-1
D87240_at*	6-Phosphofructo-2-kinase/fructose-2,6-biphosphatase 3
M64797_at	6-Phosphofructo-2-kinase/fructose-2,6-biphosphatase 4
AF038388_at	Actin-filament-binding protein frabin
S47609_s_at	Adenosine A2A receptor
M91466_at*	Adenosine A2B receptor
U90888_at	Adenosine monophosphate deaminase 3
X77235_at	ADP-ribosylation-like 4
D15069_s_at	Adrenomedullin
rc_AA866237_s_at*	Albumin
M27434_s_at	α-2u globulin PGCL1
AF030378_at	Angiopoietin-2
L36664_s_at	Angiotensin-1-converting enzyme 1
U03734_at	Angiotensin-1-converting enzyme 1
rc_AA963682_at	Ankyrin 3 (G)
X52196cds_at	Arachidonate 5-lipoxygenase-activating protein
U08986_s_at*	Aryl hydrocarbon receptor nuclear translocator
U61184_at	Aryl hydrocarbon receptor nuclear translocator
AB012600_s_at	Aryl hydrocarbon receptor nuclear translocator
M60921_g_at*	B-cell translocation gene 2, antiproliferative
U34963_s_at	Bcl2-like 1
U72350_at	Bcl2-like 1
Z22607_at	Bone morphogenetic protein 4
U35774_at	Branched chain aminotransferase 1, cytosolic
rc_AA894004_at	CAPG protein
L03201_at	Cathepsin S
S77528cds_s_at	CCAAT/enhancer binding protein (C/EBP), β
X60769mRNA_at	CCAAT/enhancer binding protein (C/EBP), β
M65149_at	CCAAT/enhancer binding, protein (C/EBP), δ
rc_AI045030_s_at	CCAAT/enhancer binding, protein (C/EBP), δ
U92803_at	CC-chemokine-binding receptor JAB61
AF087943_s_at	CD14 antigen
D29646_at	CD38 antigen
rc_AA800243_at	Cell death activator CIDEA
L33869_at	Ceruloplasmin
U17035_s_at	Chemokine (CXC motif) ligand 10
U45965_at*	Chemokine (CXC motif) ligand 2
AF004953_a_at*	Chondroadherin
X71127_g_at*	Complement component 1
M29866_s_at	Complement component 3
D17370_g_at	CTL target antigen
U44948_at	Cysteine-rich protein 2
rc_AA800784_at*	Cysteine-rich protein 61
U39207_at	Cytochrome P450 4F5
M38566mRNA_s_at	Cytochrome P450, family 27, subfamily a, polypeptide 1
rc_AI176856_at	Cytochrome P450, subfamily 1B, polypeptide 1
U09540_g_at	Cytochrome P450, subfamily 1B, polypeptide 1
AF017393_at	Cytochrome P450, subfamily 2F, polypeptide 1
M29853_at	Cytochrome P450, subfamily 4B, polypeptide 1
AF065161_at	Cytokine-inducible SH2-containing protein
rc_AA942685_at	Cytosolic cysteine dioxygenase 1
AF075383_at	Cytokine-nducible SH2-containing protein 3
rc_AI639000_at*	DEAD/H box polypeptide 36 protein
U32681_g_at	Deleted in malignant brain tumors 1
M64711_at	Endothelin 1
D29683_at	Endothelin-converting enzyme 1
U53184_at	Estrogen-responsive uterine mRNA, partial sequence
U05014_at	Eukaryotic translation initiation factor 4E-binding protein 1
U05014_g_at	Eukaryotic translation initiation factor 4E-binding protein 1
rc_AI639246_at	Extracellular link domain-containing 1
rc_AI136396_at	Farnesyltransferase β subunit
rc_AI230914_at	Farnesyltransferase β subunit
M32062_at	Fc receptor, IgG, low-affinity III
M32062_g_at	Fc receptor, IgG, low-affinity III
M35601_at	Fibrinogen, α polypeptide
M84719_at	Flavin-containing monooxygenase 1
U18982_s_at	fos-Like antigen 2

Probe set ID	Gene name
M88469_at	f-Spondin
M77694_at*	Fumarylacetoacetate hydrolase
AF061443_at	G-protein-coupled receptor 48
rc_AI029183_s_at	Gap junction membrane channel protein α1
rc_AA800786_at	GATA-binding protein 6
D13963_at	Glutamate receptor, metabotropic 6
M91652complete_seq_at	Glutamine synthetase 1
M91652complete_seq_g_at	Glutamine synthetase 1
rc_AA852004_s_at	Glutamine synthetase 1
rc_AI232783_s_at	Glutamine synthetase 1
D00680_at*	Glutathione peroxidase 3
X06150cds_g_at	Glycine methyltransferase
rc_AA963857_at	Glypican 3
U49099_at*	Golgi SNARE protein (golgi SNAP receptor complex member 1)
M12450_at*	Group-specific component
L32591mRNA_at*	Growth arrest and DNA-damage-inducible 45α
L32591mRNA_g_at*	Growth arrest and DNA-damage-inducible 45α
rc_AI070295_g_at	Growth arrest and DNA-damage-inducible 45α
AF019624_at	Growth differentiation factor 8
L13619_g_at	Growth response protein (CL-6)
M58364_at	GTP cyclohydrolase 1
rc_AA859837_at	Guanine deaminase
K01933_at	Haptoglobin
rc_AI176658_s_at	Heat-shock 27-kDa protein 1
rc_AA944397_at	Heat-shock protein 86
rc_AA891542_at	Heat-shock protein 40-3
rc_AI179610_at	Heme oxygenase 1
M62642_at*	Hemopexin
rc_AA799893_g_at	Heterogeneous nuclear ribonucleoprotein A1
rc_AA800738_at	HIV-1 Tat interactive protein, 60 kD
AB020879_at	Homer, neuronal immediate–early gene, 3
rc_AA893172_at*	Hypothetical protein
rc_AA799537_at*	Hypothetical protein D2Ertd391e
rc_AA892306_at*	Hypothetical protein FLJ12660
U17254_at	Immediate–early gene transcription factor NGFI-B
U17254_g_at	Immediate–early gene transcription factor NGFI-B
M31837_at	Insulin-like growth factor-binding protein 3
rc_AI009405_s_at	Insulin-like growth factor-binding protein 3
D00913_at	Intercellular adhesion molecule 1
D00913_g_at	Intercellular adhesion molecule 1
U68272_at	IFN-γ receptor
M34253_g_at	IFN regulatory factor 1
M34253_at	IFN regulatory factor 1
rc_AA799861_g_at*	IFN regulatory factor 7
rc_AI014163_at	IFN-related developmental regulator 1
M98820_at	IL-1β
M95578_g_at*	IL-1 receptor, type I
AF015719_s_at	IL-15
X69903_at	IL-4 receptor
M58587_at	IL-6 receptor
AJ000557cds_s_at	Janus kinase 2
U13396_at*	Janus kinase 2
U13396_g_at	Janus kinase 2
rc_AA891041_at	Jun-B oncogene
M75148_at*	Kinesin light chain 1
D12769_at	Kruppel-like factor 9
D12769_g_at	Kruppel-like factor 9
rc_AA859581_at	Late gestation lung protein 1
J02962_at	Lectin, galactose-binding, soluble 3
rc_AA943555_s_at	Linker of T-cell receptor pathways
U24652_at	Linker of T-cell receptor pathways
rc_AA946503_at	Lipocalin 2
rc_AA875620_at	LOC361797
X73371_at	Low-affinity immunoglobulin γ Fc region receptor II precursor
rc_AA892775_at	Lysozyme
rc_AI234060_s_at	Lysyl oxidase
J05495_at	Macrophage galactose N-acetyl-galactosamine-specific lectin
M64862_at*	Matrin F/G 1
rc_AI012030_at	Matrix Gla protein
X98517_at*	Matrix metalloproteinase 12
L24374_at	Matrix metalloproteinase 7

Probe set ID	Gene name
U65007_g_at	Met proto-oncogene
Z46374cds_s_at	Met proto-oncogene
rc_AI102562_at	Metallothionein
rc_AI176456_at	Metallothionein 1E (MT-1E)
rc_AA955983_at	Microsomal glutathione *S*-transferase 2
rc_AA799508_at	Microtubule-associated proteins 1A/1B light chain 3
U05784_s_at	Microtubule-associated proteins 1A/1B light chain 3
rc_AA924542_s_at	Mitogen-activated protein kinase 14
rc_AI137862_s_at	Mitogen-activated protein kinase 14
rc_AI171630_s_at	Mitogen-activated protein kinase 14
U73142_at	Mitogen-activated protein kinase 14
U73142_g_at	Mitogen-activated protein kinase 14
U91847_s_at	Mitogen-activated protein kinase 14
M94454_at	Mitogen-activated protein kinase kinase kinase 8
rc_AI169756_s_at	Mitogen-inducible gene 6 protein homolog (Mig-6) (gene 33 polypeptide)
M23572_at	Mitogen-inducible gene 6 protein homolog (Mig-6) (gene 33 polypeptide)
rc_AA943677_at	Munc13-3
AF020618_at*	Myeloid differentiation primary response gene 116
M27151_at	Myogenic factor 6
X52711_at	Myxovirus (influenza virus) resistance
D82074_at	Neurogenic differentiation 1
rc_AI072943_at	Neurotensin receptor 2
X63594cds_at	Nuclear factor of κ light chain
X63594cds_g_at	Nuclear factor of κ light chain
AF014503_at	Nuclear protein 1
AF000899_at*	Nucleoporin p58
rc_AA892598_at	Nucleostemin
rc_AI230294_at	Fanconi anemia, complementation group E
AF104362_at	Osteomodulin (osteoadherin)
V01216_at*	Orosomucoid 1
AB005900_at*	Oxidized low-density lipoprotein receptor 1
rc_AA799744_at	β-Galactosidase
rc_AA859593_at	PDB:1lbg
AB016532_at	Period homolog 2
U40064_at	Peroxisome proliferator-activated receptor δ
rc_AA893267_at	PEST phosphatase-interacting protein
D88666_at	Phosphatidylserine-specific phospholipase A1
L27059_s_at	Phosphodiesterase 4D
L27060_at	Phosphodiesterase 4D
X51529_at	Phospholipase A2, group IIA (platelets, synovial fluid)
rc_AA891751_at*	Sodium channel α-chain HBA
rc_AA800808_at*	Hypothetical protein (B2 element)
rc_AA892446_at*	Hypothetical protein (B2 element)
rc_AA799497_at	Hypothetical protein DKFZp434G162.1
rc_AA799497_g_at	Hypothetical protein DKFZp434G162.1
L40030_at	Placental growth factor
U77697_at	Platelet/endothelial cell adhesion molecule
U83895_at	Pleckstrin homology, Sec7 and coiled/coil domains 1
rc_AA891314_at	Poly(rC)-binding protein 4
X78461_at	Potassium inwardly-rectifying channel, subfamily J, member 12
X53231_at	Preoptic regulatory factor-1
U05989_at	PRKC, apoptosis, WT1, regulator
X59993_at	Probable zinc-finger protein
U03388_s_at	Prostaglandin-endoperoxide synthase 1
rc_AI639113_at	Multimerin, endothelial cell, precursor
rc_AA893664_at	TEMO
M33962_at	Protein tyrosine phosphatase, non-receptor type 1
M33962_g_at	Protein tyrosine phosphatase, non-receptor type 1
rc_AI113289_s_at	Protein tyrosine phosphatase, non-receptor type 1
rc_AI180145_s_at	Protein tyrosine phosphatase, non-receptor type 1
L19180_g_at	Protein tyrosine phosphatase, receptor type, D
L19933_s_at*	Protein tyrosine phosphatase, receptor type, D
M60103_at	Protein tyrosine phosphatase, receptor type, F
D10757_g_at*	Proteosome subunit, β type 9
AF034577_at	Pyruvate dehydrogenate kinase 4
U12187_at	Ras-related associated with diabetes
AF036548_g_at	Rgc32 protein
rc_AA900505_at	Rhob
rc_AI639465_f_at	Ring finger protein 28
rc_AI639465_r_at	Ring finger protein 28
rc_AA800245_at	RING finger protein MURF
rc_AA957003_at	S100 calcium-binding protein A8 (calgranulin A)

Probe set ID	Gene name
L18948_at	S100 calcium-binding protein A9 (calgranulin B)
rc_AI008131_s_at	*S*-Adenosylmethionine decarboxylase 1
M14656_at	Secreted phosphoprotein 1
L23088_at*	Selectin, platelet
rc_AI010453_at*	Serine (or cysteine) protease inhibitor, clade A, member 1
M24067_at	Serine (or cysteine) protease inhibitor, member 1
D00753_at	Serine protease inhibitor
AF086624_s_at	Serine threonine kinase pim3
rc_H31623_s_at	Serine/threonine kinase 2
L01624_at	Serum/glucocorticoid-regulated kinase
U25281_at	SH3 domain-binding protein CR16
U31159_s_at	SH3 domain-binding protein CR16
AF053312_s_at	Small inducible cytokine subfamily A20
D63772_at	Solute carrier family 1, member 1
S59158_at	Solute carrier family 1, member 3
L35558_s_at*	Solute carrier family 1, member 1
D82883_at*	Solute carrier family 26 (sulfate transporter), member 2
U66723_s_at	Solute carrier family 28, member 2
AB015433_s_at	Solute carrier family 3, member 2
AJ001290cds_at*	Solute carrier family 5 (inositol transporters), member 3
rc_AA860049_at	BGAL_ECOLI β-galactosidase (lactase)
rc_AA891944_at	BGAL_ECOLI β-galactosidase (lactase)
L19998_at	Sulfotransferase family 1A, phenol-preferring, member 1
L19998_g_at	Sulfotransferase family 1A, phenol-preferring, member 1
rc_AI011498_at	SWI/SNF-related, matrix-associated, actin-dependent regulator of chromatin d2
U90312_at*	Synaptojanin 2
S61868_at	Syndecan 4
S61868_g_at	Syndecan 4
rc_AI169327_at*	Tissue inhibitor of metalloproteinase 1
rc_AI169327_g_at	Tissue inhibitor of metalloproteinase 1
K02814_at*	T-kininogen
K02814_g_at	T-kininogen
L25785_at	Transforming growth factor β1-induced transcript 4
M77809_at	Transforming growth factor, β receptor 3
M80784_s_at*	Transforming growth factor, β receptor 3
X57523_g_at	Transporter 1, ATP-binding cassette, subfamily B (MDR/TAP)
rc_AI639401_at	Trichohyalin
rc_AA892333_at	Tubulin, α6; tubulin α6
rc_AA859722_at	Ubiquitin-conjugating enzyme E2G 2; ubiquitin-conjugating enzyme 7
AF047707_at	UDP-glucose ceramide glycosyltransferase
AF047707_g_at*	UDP-glucose ceramide glycosyltransferase
AF035943_at	Uncoupling protein 3
L20913_s_at	Vascular endothelial growth factor
rc_AI172247_at	Xanthine dehydrogenase
rc_AA800613_at	Zinc-finger protein 36
X63369cds_at	Zinc-finger protein 36
rc_AA800840_g_at*	EST
rc_AA866383_at	EST
rc_AA875288_at	EST
rc_AA892257_at	EST
rc_AI638994_at	EST
rc_AI639136_at*	EST
rc_AI639146_at*	EST
rc_AI639417_at	EST
rc_AI639507_at	EST
AF053988_at*	EST
AF058787_at*	EST
AF069775_at*	EST
AF069782_at	EST
AF087944mRNA_s_at	EST
D11445exon#1-4_s_at	EST
D26393exon_s_at	EST
E01789cds_s_at*	EST
E03229cds_s_at	EST
E04239cds_s_at	EST
E12159cds_s_at	EST
J02722cds_at	EST
M11794cds#2_f_at	EST
M13100cds#1_g_at	EST
M24239cds#2_f_at	EST
M64793_at	EST

Probe set ID	Gene name
M86912exon_at*	EST
rc_AA859902_at	EST
M86912exon_g_at	EST
rc_AA866240_i_at*	EST
rc_AA875032_at	EST
rc_AA893693_at*	EST
rc_AA893994_at	EST
rc_AI638955_at*	EST
rc_AI639348_at	EST
rc_AI639405_at	EST
S66184_s_at	EST
S68135_s_at	EST
S74265_s_at*	EST
S77494_s_at	EST
S78284_s_at	EST
S85184_at	EST
S85184_g_at	EST
U31160mRNA_s_at	EST
X05861exon#1-6_s_at*	EST
X07266cds_s_at	EST
X07285cds_s_at	EST
X17053cds_s_at	EST
X54686cds_at	EST
X62951mRNA_s_at	EST
X89225cds_s_at	EST
Y00396mRNA_g_at	EST
Y07534cds_s_at	EST
Z15123exon#5_s_at	EST

*Probe sets were excluded by the final ANOVA with a Tukey post-hoc test.

Bcl: B-Cell leukemia/lymphoma; BGAL: β-Galactosidase; CAPG: Capping protein (actin filament), gelsolin-like; CIDEA: Cell death-inducing DNA fragmentation factor-like effector A; CTL: Cytotoxic T lymphocyte; ECOLI: *Escherichia coli*; EST: Expressed sequence tag; GATP: Guanosine triphosphate; HBA: Hemoglobin α; MURF: Muscle-specific RING finger; NGFI: Nerve growth factor-induced protein I; PRKC: Protein kinase C; SNAP: Synaptosomal-associated protein; SNARE: Soluble N-ethylmaleimide-sensitive factor-attached protein receptor; UDP: Uridine diphosphate; WT: Wilms' tumor.

Table 2

Downregulated probe sets

Probe set ID	Gene name
rc_AI103874_at	25-kDa FK506-binding protein
D32209_at*	Acidic nuclear phosphoprotein 32 family, member A
M63282_at	Activating transcription factor 3
L10640_s_at	Activin receptor IIB
L19341_at	Activin type I receptor
AF030089UTR#1_at	Activity and neurotransmitter-induced early gene protein 4 (ania-4)
M80633_at	Adenylyl cyclase 4
U60063_at	Aldehyde dehydrogenase family 1, subfamily A2
U10894_s_at	Allograft inflammatory factor 1
rc_AI178971_at	α-Globin
rc_AI169370_at*	α-Tubulin
V01227_s_at	α-Tubulin
D87515_at	Aminopeptidase B
rc_AI112173_at	ATPase Na^+/K^+ transporting β1 polypeptide
rc_AI230614_s_at	ATPase Na^+/K^+ transporting β1 polypeptide
rc_AA799448_g_at	B48013 proline-rich proteoglycan 2 precursor
AF009329_at	Basic helix-loop-helix domain containing, class B3
rc_AI639493_at	β-Galactosidase (lactase)
X03369_s_at	β-Tubulin T β15
D88890_at*	Brain acyl-coenzyme A hydrolase
rc_AI228025_s_at	Calcitonin receptor-like
rc_AI010725_g_at*	Calnexin
rc_AI171796_at	Calpain 6
D89069_f_at*	Carbonyl reductase 1
L46791_at*	Carboxylesterase 3
J00713mRNA_at	Carboxypeptidase A1
U77933_at*	Caspase 2
U84410_s_at*	Caspase 3
rc_AA926149_g_at	Catalase
rc_AA900476_g_at	Cbp/p300-interacting transactivator, with Glu/Asp-rich carboxy-terminal domain, 2
rc_AI014091_at	Cbp/p300-interacting transactivator, with Glu/Asp-rich carboxy-terminal domain, 2
rc_AI171462_s_at	CD24 antigen
U49062_at	CD24 antigen
U49062_g_at	CD24 antigen
M57276_at*	CD53 antigen
rc_AA799538_at*	cDNA clone MGC:73009 IMAGE:6889746
X60767mRNA_s_at	Cell division cycle 2 homolog A (*Schizosaccharomyces pombe*)
rc_AA925473_g_at*	Cell division cycle 42 homolog (*Saccharomyces cerevisiae*)
rc_AI227887_at*	Cell division cycle 42 homolog (*S. cerevisiae*)
X06769cds_at*	c-*fos* oncogene
Y12009_at*	Chemokine (CC motif) receptor 5
X62894_at	Chloride channel 1
X74832cds_at*	Cholinergic receptor, nicotinic, α polypeptide 1
U33553_at	Chondroitin sulfate proteoglycan 5
M57664_g_at	Creatine kinase, brain
rc_AA859543_at*	C-Terminal-binding protein 2
L16532_at	Cyclic nucleotide phosphodiesterase 1
D14014_at	Cyclin D1
D14014_g_at	Cyclin D1
X75207_s_at	Cyclin D1
rc_AA899106_at	Cyclin D2
D16309_at*	Cyclin D3
rc_AI234146_at	Cysteine and glycine-rich protein 1
rc_AA819708_s_at*	Cytochrome c oxidase, subunit 7a 3
J03179_at	D site albumin promoter binding protein
J03179_g_at	D site albumin promoter binding protein
rc_AA875577_at	Dapper2
rc_AA892388_at	Death-associated kinase 2
D78588_at	Diacylglycerol kinase ζ
D00636Poly_A_Site#1_s_at	Diaphorase 1
rc_AA963839_s_at	Diaphorase 1
L05489_at*	Diphtheria toxin receptor
J02776_s_at	DNA polymerase β
U30186_at	DNA-damage inducible transcript 3
rc_AI235707_at*	Dynactin 4
rc_AI235707_g_at*	Dynactin 4
X54531mRNA_at	Dynamin 1
rc_AI009806_at	Dynein, cytoplasmic, light chain 1

Probe set ID	Gene name
L24051_at	Early B-cell factor (olfactory neuronal transcription factor 1)
AF023087_s_at	Early growth response 1
M18416_at	Early growth response 1
rc_AI176662_s_at*	Early growth response 1
U78102_at	Early growth response 2
AJ009698_g_at*	Embigin
U36482_at*	Endoplasmic reticulum protein 29
rc_AI233219_at	Endothelial cell-specific molecule 1
K03249_at*	Enoyl-coenzyme A, hydratase/3-hydroxyacyl coenzyme A dehydrogenase
D38056_at	Ephrin A1
rc_AA892417_at	Ephrin A1
Z54212_at	Epithelial membrane protein 1
rc_AA819500_g_at	Expressed sequence AU040575
D30666_at	Fatty acid coenzyme A ligase, long chain 3
L02529_at	Frizzled 1; frizzled
L02530_at	Frizzled homolog 2 (*Drosophila*)
rc_AA800912_g_at	General transcription factor II I repeat domain-containing 1
U36771_g_at	Glycerol-3-phosphate acyltransferase, mitochondrial
X78593_g_at	Glycerol-3-phosphate dehydrogenase 2
U07971_at	Glycine amidinotransferase (L-arginine:glycine amidinotransferase)
rc_AA892799_s_at	Glyoxylate reductase/hydroxypyruvate reductase
rc_AA875084_at	Groucho protein GRG1-L; Grg1-L
rc_AI070295_at*	Growth arrest and DNA-damage-inducible 45α
AJ131902_g_at	Growth arrest specific 7
rc_AI232374_g_at	H1 histone family, member 0
rc_AA818604_s_at	Heat-shock 70-kDa protein 1A
J05405mRNA_s_at	Heme oxygenase 2
D84418_s_at*	High mobility group box 2
rc_AI008836_s_at*	High mobility group box 2
AB017140_g_at	Homer, neuronal immediate–early gene, 1
AF093267_s_at	Homer, neuronal immediate–early gene, 1
AF093268_s_at	Homer, neuronal immediate–early gene, 1
X06827_at	Hydroxymethylbilane synthase
rc_H31802_at	Hypothetical protein (B2 element)
rc_AA800218_at*	Hypothetical protein FLJ14466
rc_AA894282_at*	Hypothetical protein FLJ20312
rc_AI639060_at	Hypothetical protein FLJ20559
rc_AI639088_s_at	Hypothetical protein KIAA0670
rc_H31665_at	Hypoxia-induced gene 1
L23148_g_at	Inhibitor of DNA binding 1, helix-loop-helix protein (splice variation)
AF000942_at	Inhibitor of DNA binding 3, dominant negative helix-loop-helix protein
rc_AI171268_at	Inhibitor of DNA binding 3, dominant negative helix-loop-helix protein
X58375_at	Insulin receptor substrate 1
M62781_at	Insulin-like growth factor-binding protein 5
rc_AI029920_s_at	Insulin-like growth factor-binding protein 5
X74293_s_at	Integrin α7
AF020046_s_at	Integrin αE1, epithelial-associated
rc_AA892314_at*	Isocitrate dehydrogenase 1
L38483_at	Jagged 1
rc_AA900503_at	Jagged 1
M19647_i_at	Kallikrein
rc_AA866404_at*	KE6a
U93306_at	Kinase insert domain protein receptor
AF071204_g_at	Kit ligand
U72353_at	Lamin B1
rc_AA946108_at	Laminin 5 α3
X76985_at	Latexin
rc_AA800844_s_at	Loxl protein
X84039_at	Lumican
AB010960_s_at*	Matrix metalloproteinase 23
D14447_at	Max
Z17223_at	Mesenchyme homeo box 2
X53054_g_at	MHC RT1 class II E-β chain mRNA, 3′ end
J03752_at	Microsomal glutathione *S*-transferase 1
rc_AI227608_s_at	Microtubule-associated protein tau
rc_AI639082_s_at*	Mini chromosome maintenance deficient 6
rc_AA874919_at*	Mismatch repair protein
D49785_at	Mitogen-activated protein kinase kinase kinase 12
M64301_at	Mitogen-activated protein kinase 6
M64301_g_at	Mitogen-activated protein kinase 6
rc_AI176689_at	Mitogen-activated protein kinase kinase 6

Probe set ID	Gene name
rc_AA891054_at	Mucin 2 precursor
AJ006295_at	Myeloid/lymphoid or mixed-lineage leukemia
rc_AA866276_at	Myeloid-associated differentiation marker
M84176_at	Myogenic differentiation 1
M24393_at*	Myogenin
rc_AI175935_at	Myosin IE
X52840_r_at*	Myosin regulatory light chain
K03468_s_at*	Myosin, heavy polypeptide 3
X04267_at	Myosin, heavy polypeptide 3
rc_AI171542_at*	NADH dehydrogenase (ubiquinone) 1β subcomplex
rc_AA799499_at*	NADH dehydrogenase (ubiquinone) 1β subcomplex 3
AA686870_f_at	NADH ubiquinone oxidoreductase
AA799336_at*	NADH ubiquinone oxidoreductase 9.6-kDa subunit
rc_AI171959_at	Neuraminidase 2
AF016296_at	Neuropilin
AF077338_at*	Norvegicus myosin-binding protein H
rc_AI102839_at	Notch 3
rc_AI102839_g_at	Notch 3
AB012230_at	Nuclear factor I/B
M25804_at	Nuclear receptor subfamily 1, group D, member 1
M25804_g_at	Nuclear receptor subfamily 1, group D, member 1
rc_AI012183_at*	Nuclear receptor subfamily 2, group F, member 2
M36074_g_at	Nuclear receptor subfamily 3, group C, member 2
rc_AI176710_at	Nuclear receptor subfamily 4, group A, member 3
rc_AA894092_at	Osteoblast-specific factor 2 precursor
rc_AI009098_at	Oxygen-regulated protein (150 kDa)
AF039832_g_at*	Paired-like homeodomain transcription factor 2
rc_AA891438_at	Pantothenate kinase 2 (PANK2)
M31603_at	Parathyroid hormone-like peptide
M19533mRNA_i_at	Peptidylprolyl isomerase A
rc_AA818858_s_at	Peptidylprolyl isomerase A
U38376_s_at	Phospholipase A2, group IVA (cytosolic, calcium-dependent)
rc_AA894345_at	Phosphoprotein enriched in astrocytes 15
D10853_at	Phosphoribosyl pyrophosphate amidotransferase
rc_AI169104_at	Platelet factor 4 precursor (PF-4) (CXCL4)
rc_AI102795_at	Pleiotropin
AB020504_at	PMF32 protein
AB020504_g_at	PMF32 protein
D42145_at	Potassium inwardly-rectifying channel, subfamily J, member 8
rc_AA799691_at	Potassium-chloride cotransporter KCC4
M24604_at*	Proliferating cell nuclear antigen
X78949_at*	Prolyl 4-hydroxylase α subunit
L02615_at	Protein kinase inhibitor, α
D14568_at*	Protein phospatase 3, regulatory subunit B, α isoform, type 1
U57499_g_at*	Protein tyrosine phosphatase, non-receptor type 11
U28938_at	Protein tyrosine phosphatase, receptor type, O
rc_AA799812_g_at	Protein-tyrosine-phosphatase (EC 3.1.3.48), non-receptor type 3
U56839_at	Purinergic receptor P2Y, G-protein-coupled 2
U82591_at	Putative c-Myc-responsive
X06889cds_at	RAB3A, member RAS oncogene family
rc_AI230406_at*	Ras-related protein Rab10
rc_AA899253_at	Rat mRNA
M81639_at	*Rattus norvegicus* stannin mRNA
U27767_at	Regulator of G protein signaling 4
rc_AI639318_at	ret proto-oncogene
AJ223083_at	Retinoid X receptor γ
M10934_s_at	Retinol-binding protein 4
X67504_at	RT1 class Ib gene(Aw2)
X06916_at	S100 calcium-binding protein A4
rc_AI228548_at	S100 protein, α chain
AF071495_s_at	Scavenger receptor class B, member 1
D89655_at	Scavenger receptor class B, member 1
rc_AA875172_at	SH3-domain kinase-binding protein 1
U81186_g_at*	Smooth muscle-specific 17β-hydroxysteroid dehydrogenase type 3
M22253_at	Sodium channel, voltage-gated, type 1, α polypeptide
AF051561_s_at	Solute carrier family 12, member 2
D63834_at	Solute carrier family 16, member 1
U17133_at	Solute carrier family 30, member 1
U76714_at	Solute carrier family 39 (iron-regulated transporter), member 1
U76714_g_at	Solute carrier family 39 (iron-regulated transporter), member 1
rc_AA875037_at	SPI6
rc_AA851749_s_at	Splicing factor, arginine/serine-rich

Probe set ID	Gene name
rc_AI231821_at	Stathmin 1
J02585_at*	Stearoyl-coenzyme A desaturase 1
rc_AI175764_s_at*	Stearoyl-coenzyme A desaturase 1
M15114_g_at	Stearoyl-coenzyme A desaturase 2
rc_AA875269_at	Stearoyl-coenzyme A desaturase 2
U67995_s_at	Stearoyl-coenzyme A desaturase 2
L27112_s_at	Stress-activated protein kinase α II
Y00497_s_at*	Superoxide dismutase 2
M81687_at	Syndecan 2
U40188_at	TAF9-like RNA polymerase II, TATA box-binding protein (TBP)-associated factor, 31 kDa
U15550_at*	Tenascin C
rc_AI071299_at	TGFB-inducible early growth response
K01934mRNA#2_at	Thyroid hormone responsive protein
rc_AA899854_at*	Topoisomerase (DNA) 2α
X62323_at	Transcription factor E2a
M61725_s_at	Transcription factor UBF
U03491_at*	Transforming growth factor, β3
M83107_at	Transgelin
rc_AI059508_s_at*	Transketolase
rc_AA891880_g_at	Tricarboxylate carrier-like protein
M60666_s_at	Tropomyosin 1, α
rc_AA875132_at	Tropomyosin 1, α
rc_AA800948_at	Tubulin α-4 chain
AB011679_at	Tubulin, β5
rc_AA800298_at	Type XV collagen
rc_AI175900_g_at	v-ets erythroblastosis virus E26 oncogene homolog 1 (avian)
rc_AA945867_at*	v-jun sarcoma virus 17 oncogene homolog (avian)
rc_AI175959_at*	v-jun sarcoma virus 17 oncogene homolog (avian)
rc_AI180108_at*	Wbscr1
rc_AI136891_at*	Zinc-finger protein 36, C3H type-like 1
rc_AA799396_at	EST
rc_AA799396_g_at	EST
rc_AA799889_at*	EST
rc_AA800768_at	EST
rc_AA800770_at*	EST
rc_AA800908_at*	EST
rc_AA859663_at	EST
rc_AA859896_at	EST
rc_AA859922_at*	EST
rc_AA866443_at	EST
rc_AA874873_g_at	EST
rc_AA891288_at	EST
rc_AA891288_g_at	EST
rc_AA891447_at*	EST
rc_AA891797_at	EST
rc_AA892294_at*	EST
rc_AA892362_at	EST
rc_AA892538_at	EST
rc_AA892986_at	EST
rc_AA893082_at	EST
rc_AA893663_at	EST
rc_AA894199_at*	EST
rc_AA894292_at	EST
rc_AA925717_at*	EST
rc_AA925762_at	EST
rc_AA955167_s_at	EST
rc_AI102620_at*	EST
rc_AI177256_at	EST
rc_AI231778_at*	EST
rc_AI638960_at	EST
rc_AI639149_s_at	EST
rc_AI639410_i_at*	EST
rc_H31418_at	EST
rc_H33001_at	EST
rc_H33426_g_at	EST
rc_H33636_at	EST
AF087839mRNA#1_s_at*	EST
AFFX-BioDn-5_at*	EST
AFFX-CreX-3_at*	EST

Probe set ID	Gene name
AFFX-CreX-5_at*	EST
D10587_at*	EST
D42137exon_s_at	EST
E06822cds_s_at	EST
J00797cds_s_at	EST
K00750exon#2-3_at*	EST
K03039mRNA_s_at*	EST
L00370cds_s_at	EST
L16995_at	EST
M15358cds_at*	EST
M34112_s_at	EST
M36151cds_s_at*	EST
M81183Exon_UTR_g_at	EST
M94918mRNA_f_at	EST
M94919mRNA_f_at	EST
rc_AA800639_at*	EST
rc_AA800701_at*	EST
rc_AA858640_s_at*	EST
rc_AA860039_s_at	EST
rc_AA874848_s_at	EST
rc_AA891962_at	EST
rc_AI010292_s_at*	EST
rc_AI639307_at	EST
rc_AI639515_at	EST
S69206_s_at	EST
S77900_g_at	EST
S82233_s_at	EST
U23146cds_s_at	EST
U75397UTR#1_s_at	EST
X03347cds_g_at*	EST
X06801cds_i_at	EST
X07551cds_s_at	EST
X12748cds_s_at	EST
X14254cds_at	EST
X14254cds_g_at	EST
X51531cds_at*	EST
X51531cds_g_at	EST
X80130cds_i_at*	EST
Z27118cds_s_at*	EST

* Probe sets were excluded by the final ANOVA with a Tukey post-hoc test.

CXCL: CXC chemokine ligand; EST: Expressed sequence tag; KE: K region expressed; MHC: Major histocompatibility complex; NADH: Nicotinamide adenine dinucleotide; UBF: Upstream binding factor.

Table 3

Biphasic probe sets

Probe set ID	Gene name
J03024_at	Adrenergic receptor, β_2
M73714_at	Aldehyde dehydrogenase family 3, subfamily A2
U50736_s_at	Ankyrin-like repeat protein
AF015953_at	Aryl hydrocarbon receptor nuclear translocator-like
rc_AA817854_s_at	Ceruloplasmin
AF030358_g_at	Chemokine (CX3C motif) ligand 1
D10262_at	Choline kinase
U36992_at	Cytochrome P450, subfamily 7B, polypeptide 1
M80367_at*	Guanylate-binding protein 2, IFN-inducible
M25350_s_at	Phosphodiesterase 4B
rc_AA799729_g_at*	Phosphodiesterase 4B
rc_AA892750_at	Regulator of G protein signaling 1
rc_AI172476_at	TGF-β-inducible early growth response
L12025_at	Tumor-associated antigen 1
AF030163_s_at	Uncoupling protein 3
M84488_at	Vascular cell adhesion molecule 1
rc_AI639056_at	EST
M64795_f_at*	EST
X17053mRNA_s_at	EST

* Probe sets excluded by the final ANOVA with a Tukey post-hoc test.

EST: Expressed sequence tag; TGF: Transforming growth factor.